



Enhancement of the Identification of Historical Timber Element's Local Stiffness Based on Resistance Drilling Measurements

Nathalie Van Roy¹(✉), Els Verstrynge¹, and Koenraad Van Balen²

¹ Civil Engineering Department, KU Leuven, Heverlee, Belgium
{nathalie.vanroy, els.verstrynge}@kuleuven.be

² Civil Engineering Department and Raymond Lemaire International Centre for Conservation (RLICC), KU Leuven, Heverlee, Belgium
koenraad.vanbalen@kuleuven.be

Abstract. Assessing aged historical timber structures' residual capacity is challenging. Attempts to relate the results of local non-destructive tests to the timber element's global behaviour have shown insufficient correlations. This research aims at enhancing the assessment of a historical timber element's global mechanical behaviour based on local non-destructive testing. The first step, presented in this paper, is the identification of the local stiffness of a timber element based on resistance drilling measurements.

An experimental test program was designed for beams in European Oak and is representative for the assessment of mechanical properties of timber elements in compression. This paper discusses the first part of the experimental test program, in which a total of 30 small samples with a cross section of 20 by 20 mm and a height of 60 mm were taken from three different timber elements. The aim is to link the results of resistance drilling measurements to the local timber stiffness. The second part of the experimental test program will investigate how to integrate the local stiffness into a Finite Element model in order to improve the numerical analysis of a timber element's global mechanical behaviour in compression.

The prediction of the timber element's residual structural capacity using NDT tests contributes to a more accurate assessment of historical timber structures and their preservation.

Keywords: Historical timber structures · Non-destructive testing
Resistance drilling measurements · Influence slope of grain
Material characterisation

1 Introduction

An approach for the assessment of the residual capacity of historical timber structures was developed within the framework of the European Cooperation in Science and Technology-Wood Science for Conservation of Cultural Heritage (COST IE0601-WoodCultHer) [1]. This approach, published as "Guidelines for the structural assessment of historic timber structures" fits within the general reference document for

historical structures' structural repair, namely the ICOMOS charter "Principles for the analysis, conservation and structural restoration of architectural heritage", ratified in 2003 [2]. The assessment approach consists of visual inspections, an understanding of the structures' history, a geometrical survey (dimensions of the elements), an understanding of the environmental conditions and a detailed survey of joints and timbers. The detailed investigation of joints and timbers focuses on a qualitative assessment and an identification of damages. The timber quality is evaluated based on the identification of the species and visual strength grading [1]. Several publications stress the difficulty in analysing the structural behaviour of historical timber structures, due to uncertainties in numerical and analytical analysis. These uncertainties are related to the geometry, the joint behaviour, and the mechanical properties of the timber elements [3, 4].

The research presented in this paper addresses the on-site assessment of the local stiffness of timber elements. The first section of the paper reports on the developed experimental test program and the experimental results of compression test on small timber samples. The second section of the paper reports on how the local timber stiffness can be determined based on non-destructive testing, with the use of resistance drilling measurements. The aim is the identification of the local Young's moduli along the material's orthotropic axes.

2 Test Program

2.1 Materials

The tests are performed on samples taken from three different elements in old timber, with a cross section of about 150×150 mm and a length of about three meters. The three elements are reclaimed antique beams in European oak (*Quercus robur*), that were purchased and proclaimed to derive from a demolished building in France. These specific elements in European oak were selected as representable for the timber elements often found in existing historical timber roof structures constructed until the 19th Century in the Flanders area. The average densities of the samples taken from the three elements, hereafter referred to as E1, E2 and E3, is respectively 731 kg/m^3 , 898 kg/m^3 , and 653 kg/m^3 . The beams are stored in controlled climate conditions (R.H. = 60%, $T = 20 \text{ }^\circ\text{C}$) for a period of one year before cutting three smaller pieces with a height of 60 mm from the elements. Piece P1 is cut from E1, piece P2 is cut from E2 and piece P3 is cut from E3. These three pieces are subsequently cut into samples with a cross section of 20 by 20 mm and a height of 60 mm. A total of 30 samples were successfully tested: 11 samples for P1, 9 samples for P2 and 10 samples for P3. The sample unit size is based on the ASTM Standard [5–7].

2.2 Test Setup

The samples are subjected to a compression test parallel to the grain. The test is carried out in displacement control using a hydraulic press (Schimadzu, maximum capacity 100 kN). Firstly, three compression cycles were performed on the samples, with a displacement rate of 0.01 mm/s until a load value P. The load P was respectively 9 kN,

9 kN and 8 kN for P1, P2 and P3. After each of the cycles the load was decreased until 1 kN. Secondly, a monotonic compression test was performed until failure occurred.

2.3 Experimental Results

The compression tests parallel to the grain allowed to determine the Young's modulus along the axes of the applied load (E_z) and the maximum compression strength parallel to the grain ($\sigma_{c,0}$) for the samples. The results are given in Table 1. The average stiffness and strength of pieces P1, P2, and P3 is in line with their average densities. The average moisture content of the samples is measured before testing them and is found to be 10.9%, which indicates the timber is at equilibrium moisture content levels and the moisture content will not influence the mechanical properties.

Table 1. Results experimental compression test parallel to the grain.

P1			P2			P3		
Sample	E_z (MPa)	$\sigma_{c,0}$ (MPa)	Sample	E_z (MPa)	$\sigma_{c,0}$ (MPa)	Sample	E_z (MPa)	$\sigma_{c,0}$ (MPa)
1.1	5789	26.64	2.1	6692	44.14	3.1	4851	25.55
1.2	8371	28.90	2.2	6358	57.98	3.2	5070	36.14
1.3	7369	39.56	2.3	4178	30.75	3.3	6726	34.06
1.4	6073	26.87	2.4	6981	49.76	3.4	6039	33.11
1.5	8259	26.59	2.5	5532	36.71	3.5	6050	30.67
1.6	9110	26.03	2.6	6675	41.66	3.6	6820	24.96
1.7	4958	39.15	2.7	5358	49.80	3.7	4641	41.13
1.8	6718	39.68	2.8	3926	36.56	3.8	3825	33.59
1.9	8229	40.71	2.9	5783	38.27	3.9	3849	37.00
1.10	8542	27.21				3.10	4007	32.95
1.11	5909	56.25						
Average	7212	34.33	Average	5720	42.85	Average	5188	32.93
$E_{z,1}$			$E_{z,2}$			$E_{z,3}$		
STDEV.	1386	9.61	STDEV.	1097	8.46	STDEV.	1153	4.93

The high variability in the test observations can be ascribed on the one hand to timber's inherent inhomogeneity and on the other hand to the test setup. The lateral restraints near the end surfaces of the samples will cause stress concentrations [8]. Since the Young's modulus is determined based on the displacement of the press head, and thus on the average vertical strain measured over the full height of the sample, this will be the cause for an inaccuracy in the determined values. Ongoing research consists of determining the vertical strain for the central area of the specimen based on Stereo-vision digital image correlation (DIC), which is an optical full-field measurement method.

3 Identification of Local Young's Moduli

The aim of the experimental investigation is to link an existing semi-destructive technique to the local Young's moduli along the orthotropic axes of the timber samples. Based on previous research into the properties of timber and the traditional use of timber elements, four main characteristics are defined that influence the mechanical behaviour of timber, namely the fibre density (strongly related to the wood species), the wood moisture content, the slope of the natural grain and the presence of defects and pathologies [9]. At a local level, the presence of defects will cause deviations in the slope of the natural grain, and changes in the fibre density. For this experimental investigation, the samples are kept in controlled climate conditions with a relative humidity of 60% and a temperature of 20 °C. Furthermore, the samples were taken from the heartwood, which did not show any sign of pathologies. Therefore, with this specific focus and under these specific conditions, there are two main characteristics that will influence the local Young's moduli: the density and the slope of the natural grain. Identifying the density should therefore allow the identification of the local mechanical properties, while the slope of the natural grain is considered an influencing parameter.

3.1 Identification of the Local Density: Resistance Drilling Measurements

European oak is a ring-porous hardwood with a clear difference in cell size between the early wood and latewood. This is due to the differences in radial dimension and cell wall thickness. The early wood is formed early in the growing season and it has a lower density and large cell cavities. The latewood is the darker portion of the growth ring and it has a higher density. Due to this distinct difference in this type of hardwood, each growth ring can be considered as a distinct layer, with its own density, stiffness, and strength [7]. Identification of the growth rings is therefore an interesting approach for determining the density of ring-porous hardwood. Resistance drilling measurements allow to determine the drilling resistance of a needle with a diameter of 1.5 mm as it penetrates a timber element. Tannert et al. indicate that if the needle is able to accurately penetrate the wood, the test enables to measure the local density at the position of the needle's tip based on the drilling resistance [10]. Acuña et al. identified a linear relation, see Eq. (1), between the densities of six types of wood (Scots Pine, Corsican Pine, Maritime Pine, Sweet Chesnut, Persian Walnut, European Oak), for samples of 100 by 100 by 150 mm, with a coefficient of determination R^2 equal to 82% [11].

$$\rho = 0.76RM_{av} + 395 \quad (1)$$

Based on these promising results from existing research and the easy applicability of the Resistograph on site, this semi-destructive testing method was considered fit for the assessment of the samples' local stiffness in the experimental test program. A RINNTECH Resistograph ® R650-SC was used to measure the drilling resistance at five positions, with a height difference of 10 mm between the measurements. These measurements were repeated in two directions, allowing for each sample to determine an average drilling resistance RM_{av} based on 20 drillings, according to Eq. (2), where $n = 20$.

$$RM_{av} = \frac{\sum_{i=1}^n RM_i}{n} \tag{2}$$

Figure 1 indicates how for piece P2 the RM_{av} for sample 2.7, indicated in red, is determined based on drilling measurements 6 to 10 and 11 to 15 from one side and drilling measurements 26 to 30 and 31 to 35 from the other side. The resistance drilling measurements are carried out in between the samples that are later cut out for compression testing.

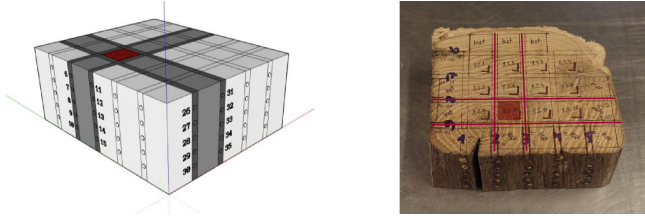


Fig. 1. Piece P2 with indication of sample 2.7 and location of drilling measurements (sample size P2: 130 × 155 × 60 mm)

The average drilling resistance RM_i for each measurement is determined based on Eq. (3). $R_{i,d}$ is the measured drilling resistance at a drilling depth d , while d_1 is the initial drilling depth of the sample and d_2 is the final drilling depth of the sample. For sample 2.7 in Fig. 1, $d_{i,1} = 25$ mm and $d_{i,2} = 45$ mm for $i = 6-15$, while $d_{i,1} = 75$ mm and $d_{i,2} = 95$ mm for $i = 26-35$.

$$RM_i = \frac{\int_{d_{i,1}}^{d_{i,2}} R_{i,d}}{d_{i,2} - d_{i,1}} \tag{3}$$

A high variability was observed in the measured drilling resistances RM_i . For P1, the average coefficient of variation (COV) of the measured drilling resistances within one drilling measurement was 25%, whereas for P2 the average COV was 35% and for P3 the average COV was 21%. The measured drilling resistance is known to be influenced by the drill bit sharpness and the drill orientation. Sharpness of the drill bit is assured by changing the needle every 100 measurements for hardwood. The influence of the drill orientation with respect to the annual rings was filtered out in post-processing by assuring a maximum coefficient of variation of 15% between the average drilling resistance RM_i for the five measurements done at five different heights. Test results that deviated from the other tests were not included in the calculation of the samples' RM_{av} . Figure 2a gives an overview of the average drilling resistance RM_{av} of the tested samples, with an indication of the standard deviation between the average drilling resistance RM_i of the measurements done for each sample. The graph demonstrates that for higher average drilling resistances the values are more spread out than for lower average drilling resistances. This could be ascribed to higher differences in density between the early wood and the latewood.

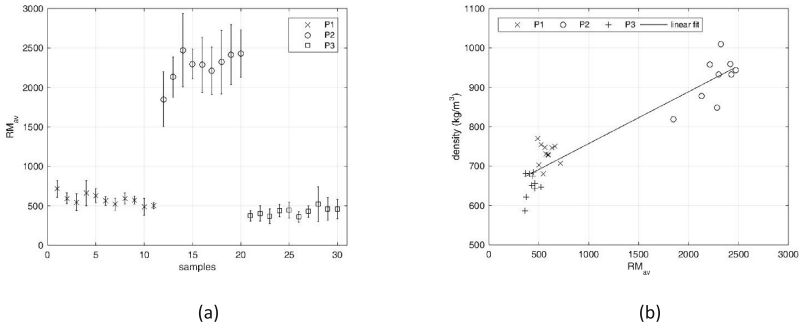


Fig. 2. (a) Overview of average drilling resistance RM_{av} of the tested samples for pieces P1, P2, P3, with error bars indicating the standard deviation between the average drilling resistance RM_i of the measurements done for each sample, (b) Scatter plot of the linear correlation between the samples' average drilling resistance RM_{av} and its density (kg/m^3). The equation of the linear fit equals $\rho = 0.13RM_{av} + 625$ and the coefficient of determination R^2 equals 0.87.

Figure 2b gives a scatter plot of the samples' average drilling resistance RM_{av} on the horizontal axes and the samples' density in kg/m^3 on the vertical axes. A good correlation was found between the calculated average drilling resistance R_{av} and the measured densities, which coincides with existing research by Acuña et al. [11]. Based on the experimental results, the linear regression equation for European oak is given by Eq. (4).

$$\rho = 0.13RM_{av} + 625 \tag{4}$$

The coefficient of determination R^2 equals 0.87. Acuña found a linear regression equation for six species that is given by Eq. (1). The slope of the equation in Eq. (1) is higher. When singling out the samples in European Oak in Acuña's test results, a more similar slope, namely a regression coefficient that equals 0.29, was found [11]. The slope of the equation is still two times the one found in Eq. (4), which could be attributed to the aging of oak. Kránitz found an increase of about 7.5% in density for aged oak in comparison with recent oak species [12]. The influence of aging on the physical and mechanical properties of timber is however difficult to determine, since the high variation of the physical and mechanical properties within a species often superimpose possible aging effects.

3.2 Influence of the Slope of the Grain

The complex internal structure of wood gives rise to its anisotropic behaviour, which entails that the physical properties differ in different directions within the material. At a macroscopic level, a distinction is made between three main directions: the longitudinal axes L along the fibres, the radial axes R along the radius of the stem and the tangential axes T. In case of a defect-free sample, the geometric axes (X, Y, Z) along which the stresses are induced coincide with the orthotropic axes (R, T, L) of the material. In this case, the material will behave as an orthotropic material and Hooke's law can be applied to define the relationship between stresses and strains with a 6 by 6 compliance

matrix \mathbf{S} . In most cases however, the two sets of axes are misaligned, which is a condition called cross grain. In case of cross grain, the Young's moduli along the orthotropic axes (R, T, L) of the material will differ from those along the geometrical axes (X, Y, Z). The latter ones are the ones recorded during the experiments. In this case, the compliance matrix should be transformed according to Eq. (5), which is the law of transformation for the orthotropic compliance parameters. \mathbf{T} is the transformation matrix that is based on the three-dimensional rotation between the two sets of axes [7].

$$\bar{\mathbf{S}} = \mathbf{T}\mathbf{S}\mathbf{T}^{-1} \quad (5)$$

The transformed compliance matrix $\bar{\mathbf{S}}$ contains the local Young's moduli E_R , E_T , and E_L , while the compliance matrix \mathbf{S} contains the Young's moduli along the geometric axes E_X , E_Y , E_Z , whereas E_Z is the one that is given in Table 1 based on the experimental results. In order to thus identify the relationship between the material's local density and local Young's modulus along the grain (E_L), The transformed compliance matrix $\bar{\mathbf{S}}$ should be determined. Existing research has demonstrated on the one hand that a three-dimensional transformation is not always reliable for wood and on the other hand, that the influence of the rotation of the ring angle, measured between the T-axis and Y-axis, is minor. The rotation of the grain angle θ will however be significant. In this case, the material's local Young's modulus along the grain E_L can be calculated using Eq. (6) [7].

$$\frac{1}{E_Z} = \frac{\cos^4\theta}{E_L} + \frac{\sin^4\theta}{E_R} + \left(\frac{1}{G_{LR}} - \frac{2\nu_{LR}}{E_L} \right) \sin^2\theta \cdot \cos^2\theta \quad (6)$$

Bodig furthermore indicates that based on experimental research, the Young's moduli along the orthotropic axes (R, T, L) are related according to these ratios [7]:

$$E_L = 1.6 \frac{E_R}{20} = \frac{E_T}{20} = \frac{G_{LR}}{14} = 9.4 \frac{G_{LR}}{140} = \frac{G_{RT}}{140} \quad (7)$$

3.3 Identification of the Local Young's Moduli Along the Orthotropic Axes

This section proposes a method for the identification of the local Young's moduli of the samples along their orthotropic axes based on the results of the resistance drilling measurements. The aim was to identify a correlation between E and RM_{av} . The method proposes to improve the correlation by determining the local Young's modulus E_L . The scatter plot for the samples' Young's modulus E_Z is given in Fig. 3a. In this case the linear fit is given by Eq. (7) and the coefficient of determination R^2 equals 0.24. Figure 3b presents the scatter plot for the local Young's modulus E_L and the linear fit for this data is given by Eq. (8), with a coefficient of determination R^2 that equals 0.01. For the tested samples, the grain angle θ varies between 1° and 17° , with an average grain angle of 5° .

$$E_Z = -0.74RM_{av} + 7576 \quad (7)$$

$$E_L = -0.15RM_{av} + 7582 \quad (8)$$

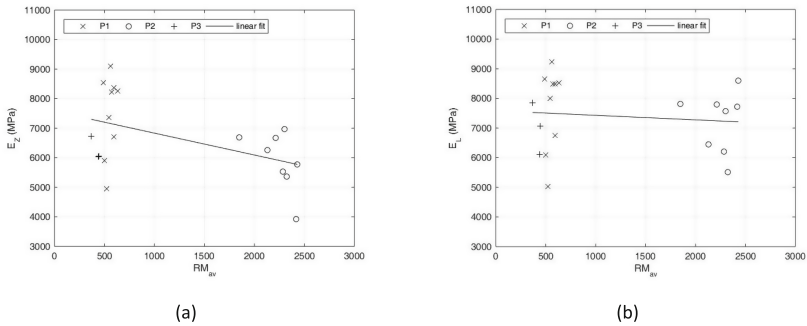


Fig. 3. (a) Scatter plot of the linear correlation between the samples' average drilling resistance RM_{av} and the Young's modulus E_Z (MPa) along the direction of the applied stresses, (b) Scatter plot of the linear correlation between the samples' average drilling resistance RM_{av} and the local Young's modulus along the grain E_L (MPa).

The scatter plots demonstrate the difficulty in determining the samples' local Young's modulus based on resistance drilling measurements. Taking into account the slope of the grain for the identification of the local Young's modulus E_L proves to be important, but is not sufficient for finding a relevant correlation. The influence of the grain angle is mostly affecting the samples with higher average drilling resistance and thus higher densities.

Based on these results, measures have been taken in the ongoing research in order to improve this correlation. Firstly, the results suggest that a more accurate determination of the vertical strain based on DIC measurements is important, since the measured Young's moduli are lower than expected for aged European Oak. Secondly, the location of the samples within the stem should be taken into account, since it will also influence the Young's moduli, which is done by testing more samples at different positions in the beam.

4 Conclusions

The difficulties in analysing the structural behaviour of historical timber structures were the grounds for setting up an experimental test program for an enhanced identification of the local stiffness based on a commonly applied semi-destructive technique, namely resistance drilling measurements. The first step of this research, presented in this paper, was a local identification of the local Young's modulus E_L . It was found relevant to start testing small samples due to the high variability that is often observed in testing of timber, due to its inhomogeneous nature and anisotropic behaviour. The experimental

results support these findings, with high coefficients of variations, even for samples taken from the same piece of a single beam. A good correlation was found between the samples' average drilling resistance RM_{av} and its density. Finding a correlation between the samples' RM_{av} and its Young modulus E_Z proved to be more challenging. Future research consists of enhancing this correlation by further elaborating the results and testing more samples at different positions in the beam.

Acknowledgments. The financial support of the Agency for Innovation by Science and Technology (IWT) for the Ph.D. grant of Nathalie Van Roy is gratefully acknowledged. The authors acknowledge the professional and practical support of L. Acuña, B. Salaets, and S. Solinas.

References

1. Cruz H et al (2015) Guidelines for on-site assessment of historic timber structures. *Int J Archit Herit* 9(3):277–289
2. ICOMOS (2003) Principles for the analysis, conservation and structural restoration of architectural heritage
3. Branco JM, Piazza M, Cruz PJS (2010) Structural analysis of two King-post timber trusses: non-destructive evaluation and load-carrying tests. *Constr Build Mater* 24(3):371–383
4. Sousa HS, Branco JM, Lourenço PB (2012) Assessment of strength and stiffness variation within old timber beams. In: Jasienko J (ed) *Structural analysis of historical constructions*. DWE, Wrocław, pp 2079–2087
5. Princes Risborough Laboratory (1974) *The strength properties of timber/The Princes Risborough Laboratory of the Building Research Establishment*. MTP Construction, Lancaster
6. American Society for Testing and Materials (1980) Standard methods of testing small clear specimens of timber, D 143–52 (72)
7. Bodig J, Jayne BA (1982) *Mechanics of wood and wood composites*. Van Nostrand Reinhold Company, New York
8. Bodig J (1969) Improved load-carrying capacity of wood in transverse compression. *Forest Prod J* 19(12):39–44
9. Van Roy N et al (2016) Quality management of structural repair of traditional timber roof structures. In: Van Balen K, Verstrynghe E (eds) *Structural analysis of historical constructions*. CRC, Leuven
10. Tannert T et al (2014) In situ assessment of structural timber using semi-destructive techniques. *Mater Struct* 47(5):767–785
11. Acuña L et al (2011) Application of resistograph to obtain the density and to differentiate wood species. *Materiales de Construcción* 61(303):451–464
12. Kránitz K (2014) Effect of natural aging on wood. In: Department of Civil, Environmental and Geomatic Engineering. ETH Zurich, Zurich